Discover Oncology

Analysis

Identification of E3 ubiquitin ligase-associated prognostic genes and construction of a prediction model for uterine cervical cancer based on bioinformatics analysis

Zhengchao Yan[1] · Jingwei Yu[1] · Shuyuan Wang[1] · Weibo Wen[1] · Mengyuan Xin[1] · Xiangdan Li[1]

Received: 9 April 2024 / Accepted: 23 August 2024
Published online: 31 August 2024

Abstract
E3 ligases are engaged in a variety of physiological processes within cells and use ubiquitin-labeled substrates to control their activity and stability. Although some research has indicated that E3 ligases or particular substrates have an impact on the treatment that cervical cancer patients get after their diagnosis, The exact purpose of these enzymes in the occurrence and evolution of cancer of the cervical region (CC) is not clear. In order to extract and analyze relevant mRNA gene expression data as well as clinical patient data, we used open databases. A reliable risk prediction model was developed by applying the least absolute shrinkage and selection operator (LASSO) technique in conjunction with Cox regression analysis. Column-line plots were combined to analyze the predictive model, and the GSE44001 dataset served as an external validation.Four gene models:proteasome (prosome, macropain) 26S subunit, non-ATPase, 14(PSMD14),proteasome (prosome, macropain) subunit, alpha type, 4(PSMA4,),zinc finger and BTB domain containing 16(ZBTB16),and ankyrin repeat domain 9(ANKRD9). Gene expression levels in both healthy and cancerous tissues have been confirmed by the HPA database. Next, the investigation focused on immunological state and tumor mutation load. The high-risk group and Cluster B had distinct levels of immune cell infiltration and a worse prognosis. Additionally, KEGG and GO analyses of differentially expressed genes (DEGs) between the high- and low-risk groups were performed, as well as tumor microenvironment (TME) investigations. Targeting E3 ligases may be an efficient strategy to treat cervical cancer (CC), according to a novel and comprehensive E3 ubiquitination ligase-associated gene model that has been presented.

Keywords E3 ligases · Cervical cancer · PSMD14 · ZBTB16 · PSMA4 · ANKRD9

1 Introduction

In terms of incidence and death, cervical cancer ranks fourth among cancers that affect women globally [1]. A recent research states that over 300,000 deaths are attributed to Cervical squamous cell carcinoma and endocervical adenocarcinoma(CESC) each year, with developing nations accounting for around 85% of these deaths [2].Cervical cancer is primarily caused by HPV infection [3]. CESC progresses through a range of complex, sequential processes, from oncogenic HPV infection, squamous cervical intraepithelial neoplasia (CIN), and in situ carcinoma to malignant

Supplementary Information The online version contains supplementary material available at https://doi.org/10.1007/s12672-024-01271-y.

✉ Xiangdan Li, lixiangdan@ybu.edu.cn | [1]Department of Morphological Experiment Center, Medical College of Yanbian University, No. 977, Gongyuan Road, Yanji 133000, Jilin, China.

development and invasion [4]. HPV DNA testing is the recommended screening approach for cervical cancer because it can accurately detect molecular and protein indicators, such as p16 immunostaining, DNA methylation, and HPV mRNA tests, which increase the specificity of the screening process [5]. Many aspects of the pathophysiology of cervical cancer remain poorly understood, and many of the biomarkers that identify the various phases of cervical carcinogenesis have unclear activities [6]. Thus, more alternatives for the early detection of CESC will become available with the ongoing research into new biomarkers.

The mammalian ubiquitination response has been linked to over 600 E3 ligases [7]. The activity of ubiquitin ligases (E3s), which control homeostasis, metabolism, the cell cycle, and several other cellular functions in the human body, is necessary for cellular responses to external signals and DNA damage.To accomplish ubiquitination, E3s identify and engage in temporal and spatial interactions with protein substrates. An E3 imbalance in cancer is indicated by both genetic and epigenetic modifications. Changes in the stability and activity of the E3 ligase can cause oncogenic activity to occasionally be down-regulated and up-regulated [8]. Based on their structure and function, they can be grouped into four families: the U-box E3 ligases, the RING in-between-RING (RBR) E3 ligases, the particularly remarkable distinctive gene (RING) finger family, and homologous to the E6-associated protein carboxyl terminus (HECT) domain family. In several signaling pathways, ubiquitination of important proteins is essential to the development of cancer of the colon. Examples include p53 [9], nuclear factor kappa-B (NF-κB) [10], epidermal growth factor receptor (EGFR) [11], Wnt/β-catenin [12], and the TGF-β/Smad pathway [13]. Increasing evidence suggests that a number of E3 ligases have been implicated as tumour suppressors in CC, and that alterations in oncogenic substrates caused by frequent mutations are the cause of cancer. Consequently, neoadjuvant treatments for CC may involve the creation of matching E3 analogues or inhibitors that target their substrates. Cancer treatments that target E3 ligases may be able to assist patients become less resistant to current treatments and may also help make tumor cells more sensitive to therapeutic drugs [14]. As an illustration ME-BS's inhibitory action on CC offers a fresh method for influencing the intrinsic ubiquitin ligase activity. A unique drug-binding method was created by Pavlides et al. to determine the activity of many SMIs of SCFSkp2/Cks1 E3 ligase (Skp2E3LIs) [15]. Furthermore, the first PROTAC small molecule with strong cellular permeability and biostability was reported by Crews et al. to be able to trigger the ubiquitination degradation of androgen receptors (ARs) in CC cells at a concentration of 10 mm [16].Thus, the development of therapeutic strategies depends on the identification of therapeutic targets for novel medications.

Consequently, we developed a predictive model connected to E3URG [17]. Next, we looked into the connection between CC immune status and two of the model's subgroups. The purpose of this work is to demonstrate how E3 ligases impact CC patients' chances of surviving and to provide fresh understanding into targeted therapy for the disease.

2 Materials and methods

Gathering and analyzing data from RNA sequencing transcriptomicsThe RNA sequencing transcriptomics data and pertinent clinical data were obtained by consulting the Cancer Genome Atlas (TCGA, https://portal.gdc.cancer.gov). Totally 307 CESC patient mRNA expression profiles and corresponding clinical data were obtained, which included 306 tumor tissues and 3 paired adjacent tissues.Clinical information was gathered, including tumor, lymph node, and metastasis (TNM) staging, as well as age, gender, and grading (Table S1). Through screening of the UniProt database (https://www.uniprot.org/), we were able to identify 1142 reviewed E3URGs. For further research, we took expression data for 1142 PRGs from of the TCGA CESC cohort.The GEO dataset, available at https://www.ncbi.nlm.nih.gov/geo/, includes clinical and RNA-seq data for 300 tumor specimens. Table S2 affords a summary of the genes that were looked up. Since data is from public databases, study is exempted from ethical review and does not need informed consent from patients.

2.1 Identification of differentially expressed genes of interest in CESC

Using R's "limma" computer package, it was possible to determine how differently E3URGs were expressed in CESC compared to nearby normal tissues (R version 4.3.1).The following criteria were used to screen E3URGs from the TCGA dataset for prognostically important genes before they were included in a one-way model. These were the significant criteria that were used: absolute $|\log2FC| > 1$, false discovery rate (FDR) < 0.05. Using the "vioplot" R package, volcano plots and heatmaps were made to show the differences in E3URG expression between CESC and nearby normal tissue samples.

2.2 Consensus clustering of several molecular isoforms of differentially expressed genes (E3URGs) associated to ubiquitin ligase

Prognostically important E3URGs were screened for using one-way Cox regression analysis. Two distinct subtypes, C1 and C2, were identified from the CESC cohort using the R package "ConsensusClusterPlus". Delta area and consensus CDF were utilized to calculate the ideal typing for 2. Based on what was found of the Kaplan–Meier analysis, survival curves have been designed to compare the overall survival (OS) of the two separate groups. The chi-square test was employed to identify variations in the clinical data (such as grading, age, and survival status) of the patients between groups.

2.3 Assessment and validation of prognostic significance

We utilized multivariate Cox regression analysis to determine the connection between E3URGs and OS. Data on cervical cancer from the TCGA database were divided into training and test sets 100 times at random. Using the least absolute shrinkage and selection operator (LASSO) regression model, fewer candidate genes were found, leading to the generation of a prediction model using the R package "glmnet". Ultimately, the minimal criterion was utilized to establish the penalty parameter (λ), and four genes together with their coefficients were kept. We multiplied the expression of genes derived from the LASSO Cox regression by its coefficient to determine the risk score.Risk Score = ∑Coefi * Xi (Coefi: the regression coefficient, Xi: gene expression value).Furthermore, the "Boruta" software package was utilized to conduct principal component analysis (PCA) for the downscaling analysis between these subgroups. Based on their median risk score, patients with CESC were allocated into low-risk and high-risk classifications. We used Kaplan–Meier analyses with the "survival", "survminer", and "timeROC" R30 values to compare OS between the two subgroups in order to validate the usefulness of the prognostic model. R packages 30, 31, 32 for ROC curve analysis include "timeROC." Calibration plots were used to assess the agreement between the estimated and real 1-, 3-, and 5-year survival probabilities. After comparing the built models to those described in earlier articles, the models were cycled to determine each model's C-index value and plotted on a histogram that represented the C-index.

2.4 Construction of projected line graphs

A prognostic column chart based on the R package "rms" was made to predict OS in CESC patients using clinically relevant variables (age and histological grade) and risk scores.

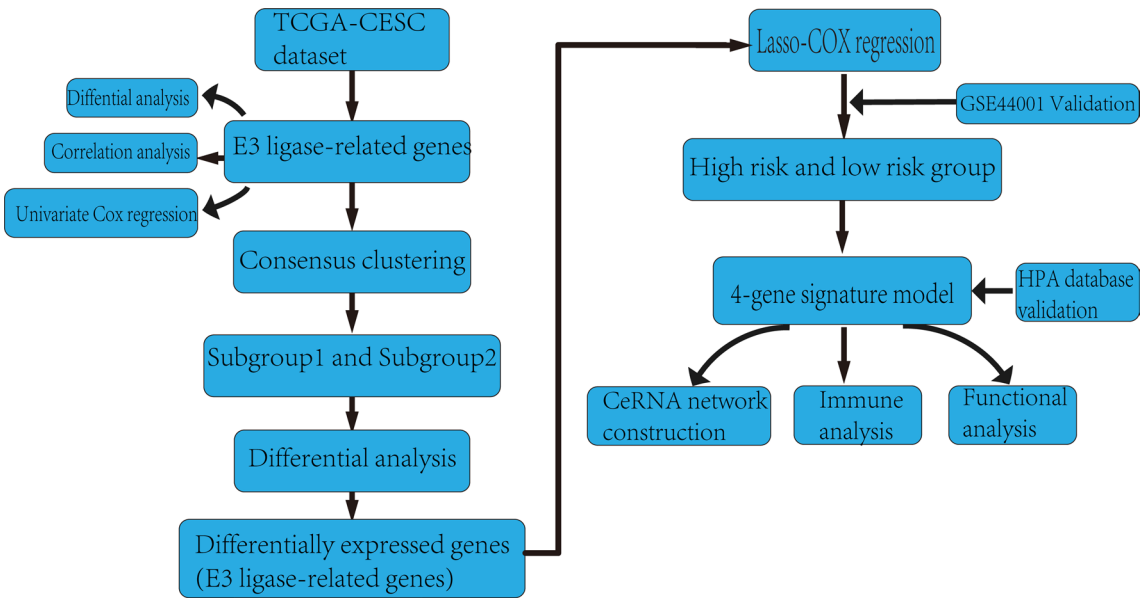

Fig. 1 Flowchart of the development and validation process for data collection and analysis [17]

Fig. 2 Expression patterns in CESC of genes associated to E3 ubiquitination ligase. Plot of a volcano displaying E3URG in CESC (**A**). Red ▶ genes are up-regulated, and green genes are down-regulated. Genes without a substantial difference are indicated by black dots. **B** A heatmap visualization showing each sample's E3URG expression levels. "Tumor" denotes samples of tumors, and "Normal" denotes normal samples. Red denotes strong expression, and green denotes modest expression. **C** A forest plot utilizing univariate Cox regression analysis for 19 E3URGs. **D** Prognostic network map and study of gene correlation

2.5 Construction of the ceRNA regulatory network

According to the ceRNA theory, some lncRNAs compete with specific target miRNA binding sites, which in turn affects mRNA expression indirectly [18, 19]. The following procedures were followed in order to develop the ceRNA regulation network based on this concept. We predicted the miRNAs of the model genes we built using miRDB (http://www.mirdb.org/), miRWalk (http://mirwalk.umm.uni-heidelberg.de/), miRanda (http://mirtoolsgallery.tech/mirtoolsgallery/node/1055), and TargetScan (version 7.2) (http://www.targetscan.org/vert_72/).Reliable target genes were those that were simultaneously predicted by all four databases. Following cross-analysis of DE mRNAs and projected target genes, overlapping mRNAs were used in additional investigation. Then, in order to create lncRNA-miRNA-mRNA ceRNA regulatory networks, additional integration studies of lncRNA-miRNA and miRNA-mRNA couples were carried out and visualised using Cytoscape (https://cytoscape.org/).

2.6 Gene set enrichment analysis

Functional enrichment research has been carried using the Kyoto Encyclopedia of Genes and Genomes (KEGG) and Gene Ontology (GO) in order to investigate and identify the underlying mechanisms. Adjustments indicate significant differences $P < 0.05$.

2.7 Analysis of immune posture

We used the coefficient "R" to compare the infiltration levels of 22 different immune cell types between the high-risk and low-risk categories. The TME of the high- and low-risk subgroups was assessed using the ESTIMATE algorithm with the "Estimate" function in terms of StromalScore, ImmuneScore, and ESTIMATEScore.

2.8 Immunochemical validation based on the HPA database

The Human Protein Atlas (HPA, http://www.proteinatlas.org/) immunohistochemical data were utilized to confirm the protein expression levels of four genes that are prognostically relevant between CESC and normal cervical samples from the TCGA cohort.

2.9 Statistical techniques

R program (version 4.2.) was used to conduct statistical analysis. The thresholds for statistical significance were $p < 0.05$ and $FDR < 0.05$. We built E3URGs with the regression model LASSO-Cox. Using Wilcoxon or paired t-tests, immune checkpoints, immune cells infiltrating cancerous tumors, immune expression, and immune function were all searched for. Kaplan–Meier analysis was used to compare OS between groups.Using transient ROC analysis, the models' predictive ability was evaluated. Spearman correlation analysis was utilized to investigate the links between immune cell infiltration and risk score. The analysis of Cox regression was employed to identify independent factors (Fig. 1).

3 Results

3.1 Finding E3URGs that are differentially expressed in CESCs

1142 E3URGs were examined for differences in expression between normal neighboring samples ($n = 3$) and CESC ($n = 306$). Between CESC and normal neighboring samples, there was a differential expression of 148 E3URGs, as

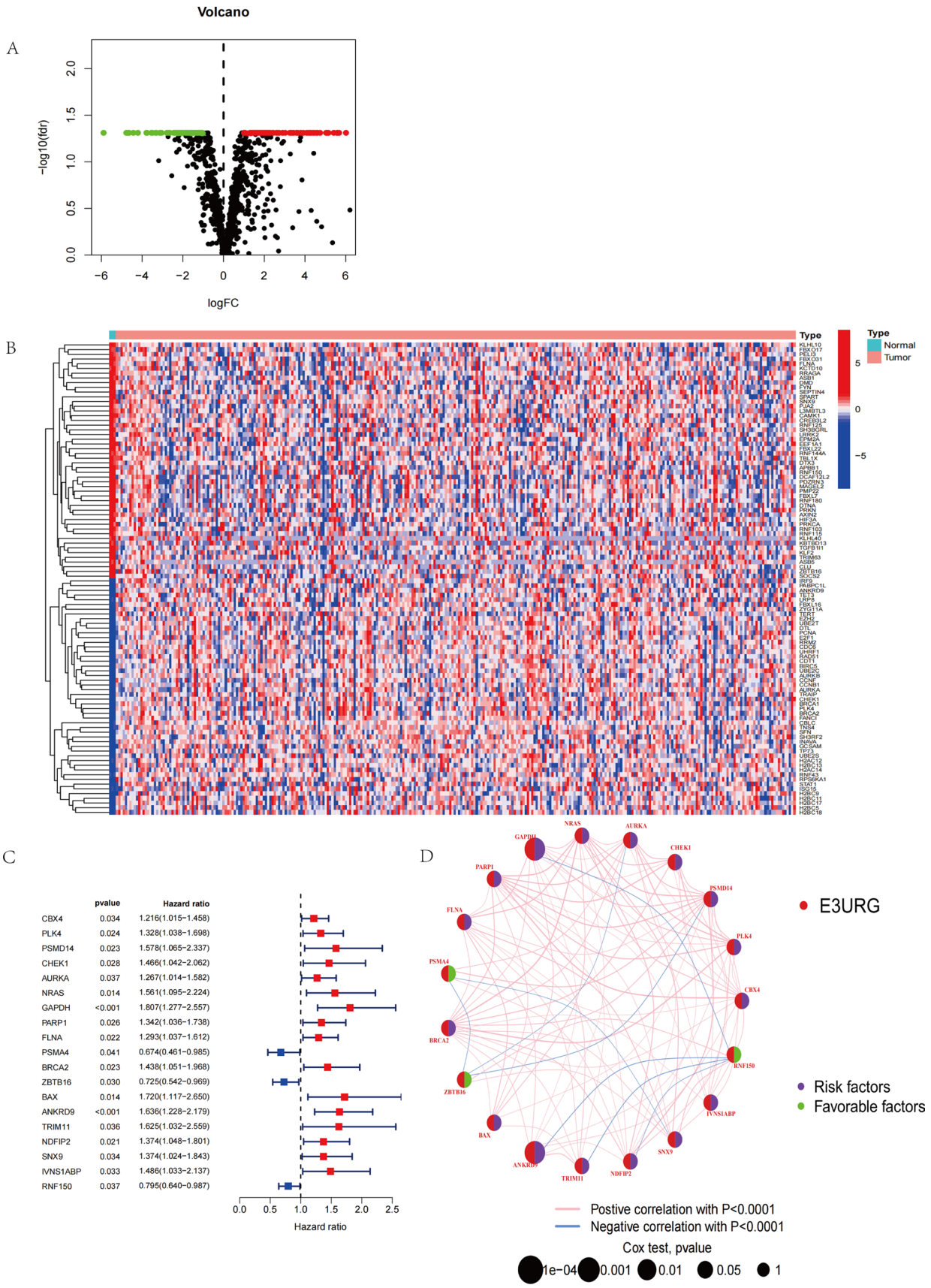
A
Volcano
−log10(fdr)
logFC
B
Type
Normal
Tumor
C
pvalue
Hazard ratio
CBX4 0.034 1.216(1.015−1.458)
PLK4 0.024 1.328(1.038−1.698)
PSMD14 0.023 1.578(1.065−2.337)
CHEK1 0.028 1.466(1.042−2.062)
AURKA 0.037 1.267(1.014−1.582)
NRAS 0.014 1.561(1.095−2.224)
GAPDH <0.001 1.807(1.277−2.557)
PARP1 0.026 1.342(1.036−1.738)
FLNA 0.022 1.293(1.037−1.612)
PSMA4 0.041 0.674(0.461−0.985)
BRCA2 0.023 1.438(1.051−1.968)
ZBTB16 0.030 0.725(0.542−0.969)
BAX 0.014 1.720(1.117−2.650)
ANKRD9 <0.001 1.636(1.228−2.179)
TRIM11 0.036 1.625(1.032−2.559)
NDFIP2 0.021 1.374(1.048−1.801)
SNX9 0.034 1.374(1.024−1.843)
IVNS1ABP 0.033 1.486(1.033−2.137)
RNF150 0.037 0.795(0.640−0.987)
Hazard ratio
D
E3URG
Risk factors
Favorable factors
Postive correlation with P<0.0001
Negative correlation with P<0.0001
Cox test, pvalue
1e−04
0.001
0.01
0.05
1

Fig. 3 Subtypes related to the E3 ligase gene were identified via consensus cluster analysis. **A**, **B**, **C** Two subgroups, A and B, can be established from TCGA cervical cancer specimens; two is the perfect number to use. **D** The overall survival (OS) K-M survival curves for subgroups **A** and **B**. **E** Heatmap showing each subgroup's age, grade, TMN, and E3 ligase-related gene expression

demonstrated by volcanograms (Fig. 2A) and thermograms (Fig. 2B).While ZBTB16, TRIM63, and PDZRN3 were expressed at low levels in normal tissues, SFN, H2BC9, and H2BC17 were expressed at significant levels in CESC tissues. Nineteen E3URGs were found using one-way Cox regression analysis (Fig. 2C). Furthermore, correlation analysis revealed that the majority of the genes have relationships with one another (Fig. 2D).

3.2 Using consensus clustering, two molecular subtypes were found

An examination of one-way Cox regression revealed 19 E3URGs. Based on the expression similarity, k = 2 demonstrated the best clustering stability from k = 2 to 9 in order to further explore the clinical importance of E3URGs (Fig. 3A, B). Based on gene expression, two subgroups of CESC patients were identified (Fig. 3C). Group A was shown to have a much better prognosis than group B based on the findings of the survival study (Fig. 3D). This heatmap illustrates the differences in the expression of pertinent clinical information across subtypes A and B, such as age, TMN, and tumor grade (Fig. 3E).

3.3 Construction of E3 ligase gene-related prognostic model

One-way Cox regression analyses were conducted on the expression levels of 148 E3URGs, based on the association seen between these regulators and OS in CESC patients.A training set and a test set were created by randomly grouping the cervical cancer data in the TCGA database 100 times. LASSO regression analysis and multivariate Cox regression analysis were run on the training cohort in order to remove overfitting from this model. Consequently, the method successfully determined the most predictive markers and produced prognostic indicators for the prediction of clinical outcomes (Fig. 4A, B). The disparity in distribution between the two risk groups was displayed by the PCA plot (Fig. 4C). Four genes were found to have the greatest significant prediction capacity based on the results (Fig. 4D). Therefore, the corresponding coefficient risk score = (0.54 × PSMD14)—(0.74 × PSMA4)—(0.42 × ZBTB16)—(0.021 × expression value of RADD) + (0.54 × ANKRD9) To find out if the risk score was an accurate marker of CESC regardless of the other clinicopathological traits, multivariate Cox regression analysis was carried out. The results from the study showed that OS along with the risk score demonstrated an independent correlation. (Fig. 4E, $P < 0.01$).

3.4 Survival analysis and ROC curve based on prognostic modelling

The prognostic value of the risk score was demonstrated by the time-dependent ROC curves, and the OS rate in the high-risk group was significantly smaller than that in the low-risk group. According to Fig. 5A, the AUC values for the test cohorts were 0.676 after one year, 0.700 after three years, and 0.698 after five years. Next, we took advantage of the GSE44001 dataset to review our risk model's accuracy in predicting in these validation cohorts [20] (Fig. 5C). The TCGA cohort's thresholds were used to divide the patient population into low- and high-risk categories. Survival studies discovered that the high-risk group maintained a lower OS rate than the low-risk group. This enhanced OS was consistent with the TCGA cohort's findings. The 1-year OS has an AUC of 0.694, the 3-year OS of 0.730, and the 5-year OS of 0.702. These outcomes confirmed the risk model's ability to predict outcomes (Fig. 5B). We examined how different clinicopathological variables affected the risk ratings within and between subgroups (Fig. 5D).

3.5 Construction of the column-line diagram

This work provides a thorough prognostic column chart based on tumor grading and risk scores (Fig. 6A) to aid in the clinical application of risk models. For LUAD patients, the column charts correctly predicted the 1-, 3-, and 5-year OS.Furthermore, the performance of the column charts was evaluated using correction curves (Fig. 6B). The study's findings showed that the model could correctly forecast OS in patients with CC.

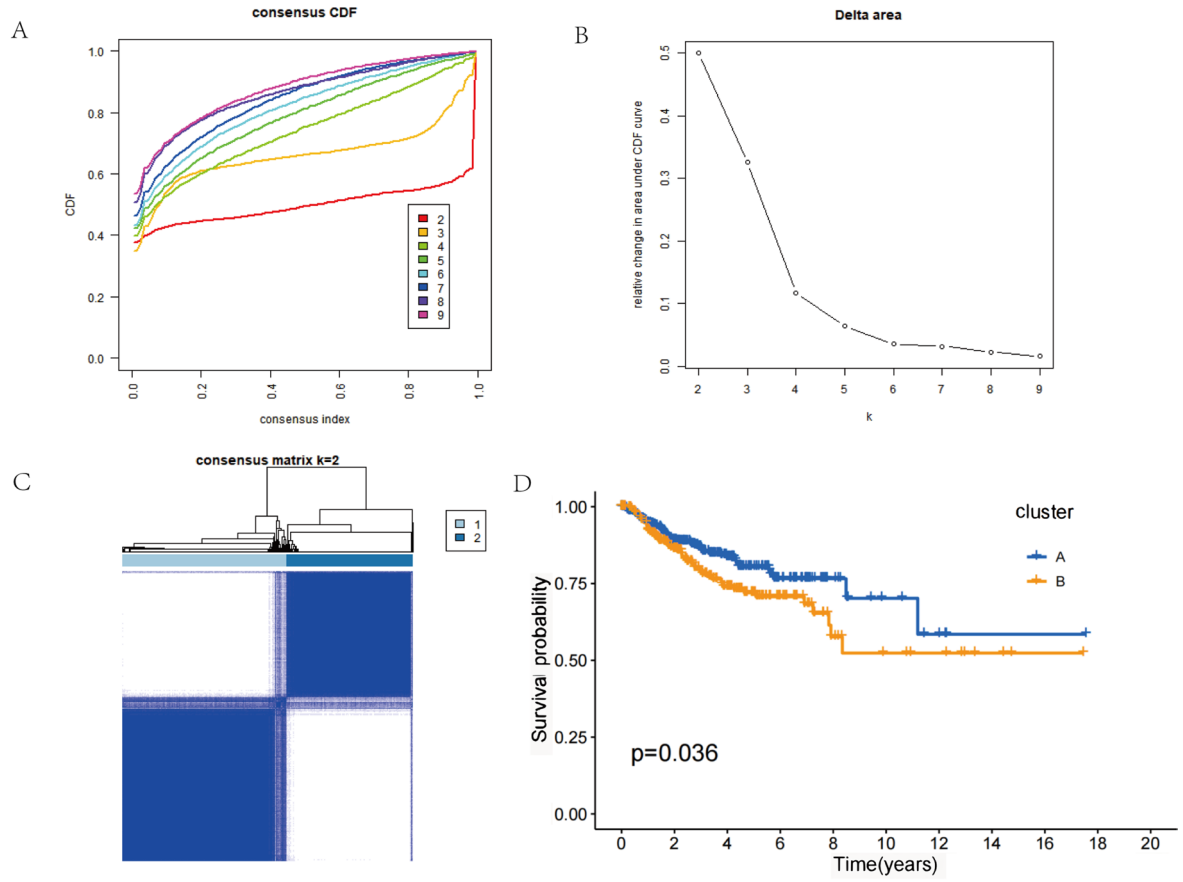
A
consensus CDF
CDF
consensus index
2
3
4
5
6
7
8
9
B
Delta area
relative change in area under CDF curve
k
C
consensus matrix k=2
1
2
D
cluster
A
B
Survival probability
p=0.036
Time(years)
E
N
M
T
Grade
Age
Project
E3URGclus
ter
CBX4
ANKRD9
TRIM11
NDFIP2
SNX9
IVNS1ABP
PARP1
AURKA
CHEK1
NRAS
PLK4
BRCA2
FLNA
PSMD14
GAPDH
PSMA4
BAX
ZBTB16
RNF150
N0
N1
unknow
M0
M1
T1
T2
T3
T4
G1
G2
G3
<=65
>65
TCGA

Fig. 4 Patients with cervical cancer had their risk markers gathered from the TCGA database. **A**, **B** Building the signature with Cox regression's absolute shrinkage and selection operator (LASSO). **C** Cervical cancer PCA plot according to risk score. **D** The four genes' coefficients that make up the signature. **E** Multivariate analysis of OS and clinicopathological characteristics using Cox regression

3.6 CeRNA network construction

Using the miRanda, miRDB, miRWalk, and TargetScan databases, gene target miRNAs were predicted for each of the four [21]. After cross-tabulating the anticipated hsa-miR-1237-3p and DEmRNAs, six mRNAs in total were found. Two miRNAs (has-miR-1297-3p, hsa-miR-205-5p), two mRNAs, and six lncRNAs were obtained through the integration of lncRNA-miRNA pairs and miRNA-mRNA couples (Fig. 7).

3.7 Differential gene enrichment study using GO and KEGG

GO and KEGG enrichment analyses were performed on DEGs linked with E3 ubiquitination ligase (Fig. 8A and B). Biological function (BP), cellular component (CC), and molecular function (MF) were the three areas with the greatest GO enrichment values. BP was primarily selected for the ubiquitin-dependent protein catabolic process mediated by proteasomes in our experiment. Proteasome complex and endopeptidase complex were the key areas of enrichment for CC, while MF was largely enriched for endopeptidase activator activity, K63-linked deubiquitinase activity, proteasome binding, and ubiquitin ligase-substrate adaptor activity. Proteasome, Prion disease, Pathways of neurodegeneration—many illnesses, and Acute myeloid leukemia were among the disorders in which KEGG was considerably enriched. leukemia exhibited considerable richness.

3.8 Analysis of the correlation between cervical cancer risk score and immune infiltration

Using the "limma" program, we were able to acquire a differential analysis of 22 distinct types of immune cells in cervical cancer between the low and high risk groups of subtypes A and B. Investigations discovered that the high-risk group's CD8T cell expression substantially lower, T cells with CD4 memory activation, resting mast cells, and neutrophils than the low risk group (Fig. 9A). This shows that patients' survival times may be somewhat impacted by the quantity of immune cells present in their cervical cancer. Scatter plots of correlation have been produced through the use of stem cell analysis on the patient risk scores (Fig. 9B). Following on the ESTIMATE strategy of the "estimate" R package, the expression levels of ImmuneScore, StromalScore, and ESTIMATEScore were drastically greater in the group with low risk in comparison to the high-risk group of participants (Fig. 9C).

3.9 Validation results are consistent with the trends expressed in the risk prediction models

According to IHC data, PSMD14 expression was more prominent in CC specimens than in normal specimens, although ZBTB16 and PSMA4 expression was decreased in tumor tissues. AnKRD9 expression was low and did not significantly differ in either tumor or normal tissue. (Fig. 10).

4 Discussion

The ubiquitin–proteasome system (UPS), which establishes substrate selectivity, depends on ubiquitin ligase E3 [22]. The UPS is responsible for the post-translational modification known as ubiquitination, which occurs when ubiquitin is linked to substrate proteins to control protein stability and localization [23]. Three distinct enzymes are involved in the process: ligases, conjugating enzymes, and enzymes that activate ubiquitin. The main circuit tactic for individualized management of E3 ligase deficiency is the creation of SMI.Improvements in PROTAC technology have facilitated the synthesis of inhibitors for targeted E3 ligases and opened up new avenues for drug development and study [7]. Recent research has found indicators associated with cancers, and the relationship between E3 ligases and malignancies is currently under investigation. Li et al., for instance, discovered that GFPT1 stimulated PTEN ubiquitination and destruction. PTEN silencing reversed the GFPT1 knockdown-induced growth suppression of cervical carcinoma [24]. Although this

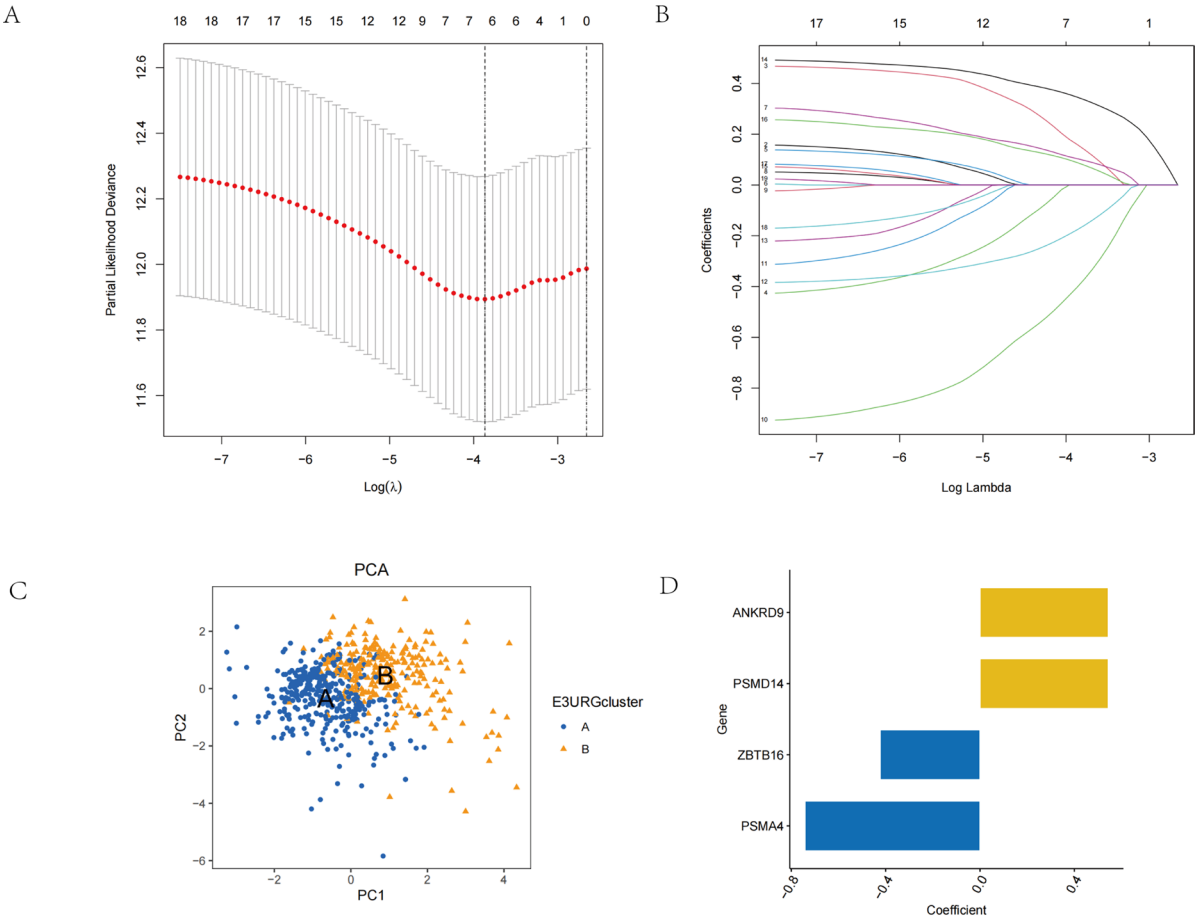
A
18 18 17 17 15 15 12 12 9 7 7 6 6 4 1 0
Partial Likelihood Deviance
Log(λ)
B
17 15 12 7 1
Coefficients
Log Lambda
C
PCA
PC2
PC1
E3URGcluster
A
B
D
ANKRD9
PSMD14
ZBTB16
PSMA4
Gene
Coefficient

E

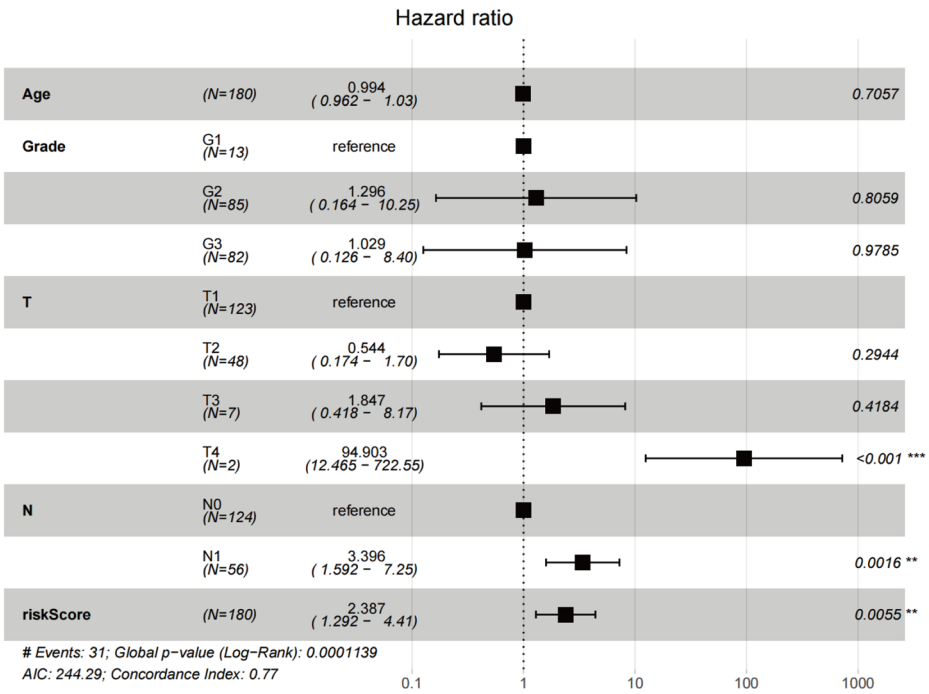
Hazard ratio
Age (N=180) 0.994 (0.962 - 1.03) 0.7057
Grade
G1 (N=13) reference
G2 (N=85) 1.296 (0.164 - 10.25) 0.8059
G3 (N=82) 1.029 (0.126 - 8.40) 0.9785
T
T1 (N=123) reference
T2 (N=48) 0.544 (0.174 - 1.70) 0.2944
T3 (N=7) 1.847 (0.418 - 8.17) 0.4184
T4 (N=2) 94.903 (12.465 - 722.55) <0.001 ***
N
N0 (N=124) reference
N1 (N=56) 3.396 (1.592 - 7.25) 0.0016 **
riskScore (N=180) 2.387 (1.292 - 4.41) 0.0055 **
Events: 31; Global p-value (Log-Rank): 0.0001139
AIC: 244.29; Concordance Index: 0.77
0.1
1
10
100
1000

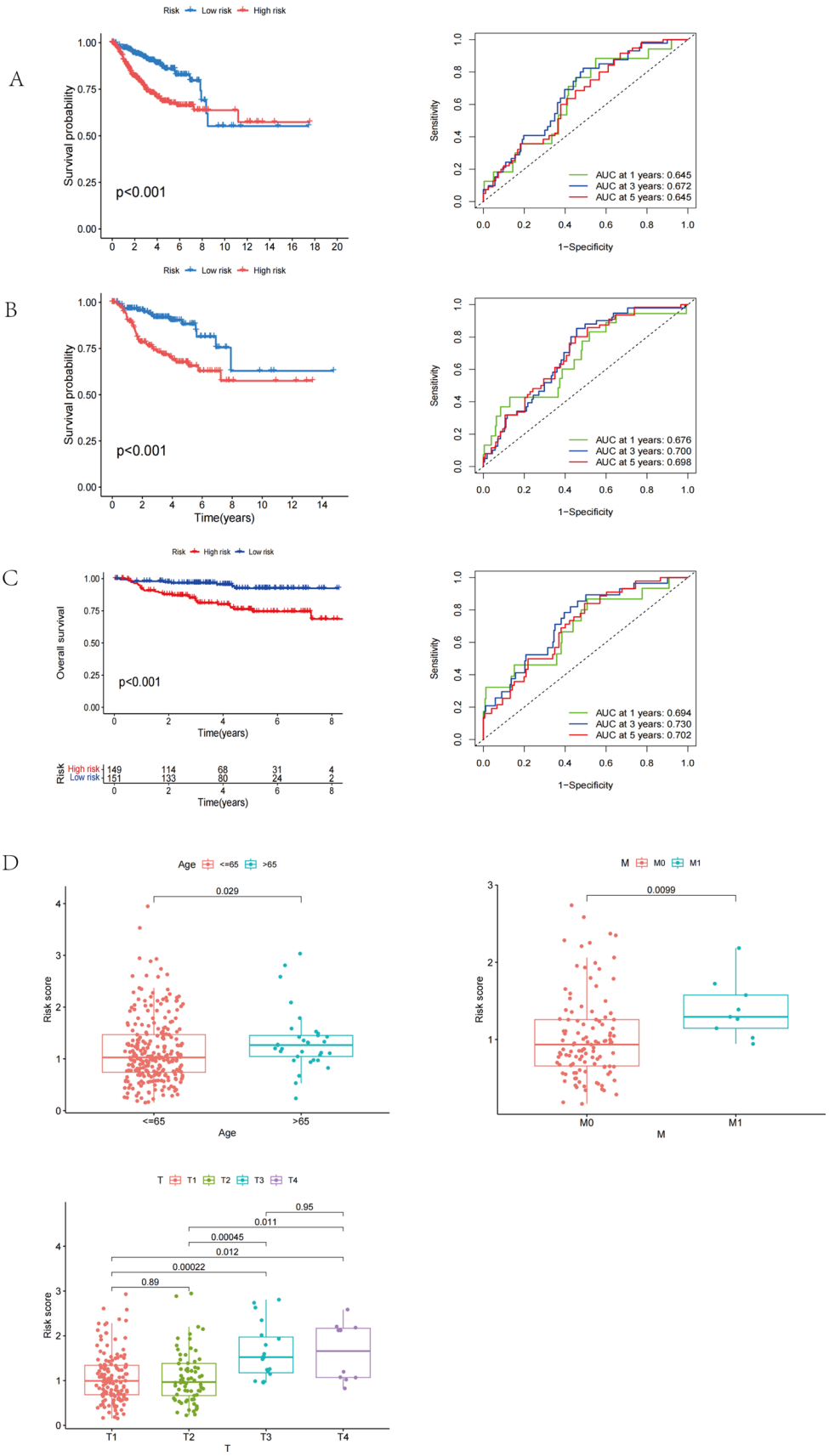

Fig. 5 Gene signatures relevant to E3 typing: construction and validation. **A**, **B**, **C** ROC curves at 1, 3, and 5 years for the training set, validation set, and GEO cohort; K-M survival curves for the high-risk and low-risk groups in each of these sets. **D** Variations in risk scores among subgroups characterized by distinct clinicopathological features. (*P < 0.05; **P < 0.01; ***P < 0.001; ns, not significant)

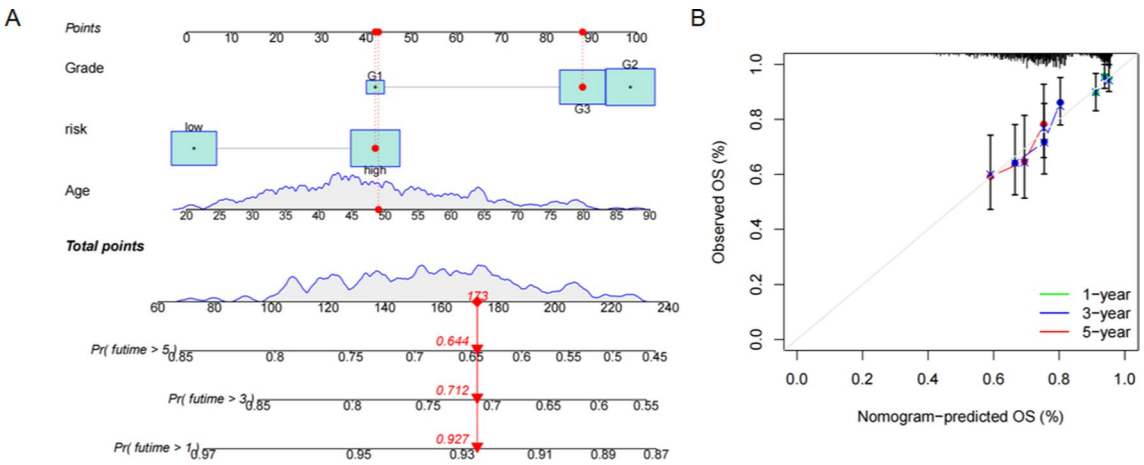

Fig. 6 Development and verification of a prognostic model for patients with cervical cancer. **A** For BC patients, 1-, 3-, and 5-year OS may be consistently predicted by merging clinical data with prognostic columnar plots. **B** Columnar plot calibrations that are used to forecast the likelihood of survival at one, two, three, and five years

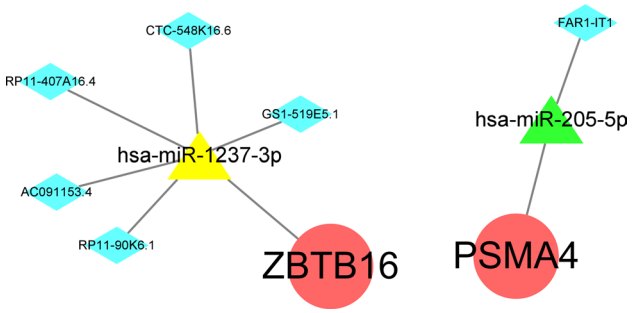

Fig. 7 The ceRNA regulatory network. **A** lncRNA-miRNA-mRNA ceRNA network

is a scarcity of oncological research on E3 ligases, bioinformatics analysis can provide useful details for upcoming basic and clinical research activities.

Our study found that a model with four genes (PSMD14, PSMA4, ANKRD9 and ZBTB16) had high specificity and sensitivity in identifying cervical cancer prognosis. KEGG and GO enrichment analysis were employed for looking into the probable biologic functions of E3URGs in CESC. Models associated with cervical cancer were developed using the selection operator (LASSO) algorithm and Cox regression analysis. We used the E3URG models to calculate risk scores and autonomously predict outcomes in CESC patients. In addition, we developed prognostic column-line plots incorporating clinical characteristics and risk scores. One-, three- and five-year survival rates were used to illustrate the validity of prognostic prediction based on column-line plots, and these results were validated in the TCGA and GEO datasets. In the final analysis, this study reveals the prognostic model's predictive validity and offers in-depth validation of the model's validity making use of a selection of tools. The risk profiles found in this study can aid in assessing the likelihood of survival for doctors. Furthermore, our investigation pointed out a robust connection of somatic mutations and E3URG's immune function microenvironment in CESC. In extra to upgrading clinical predictions, our risk model is capable of determining the extent of immunological disorders infiltration.

In this study, ANKRD9 and PSMD14 expression was elevated in CESC patients, while PSMA4 and ZBTB16 expression was reduced. In a study by Lee's people, ANKRD9 was found to be a previously unidentified E3 substrate receptor subunit that plays a role in the inhibition of gastric cancer by recognising the IMPDH isoform of the oncoprotein IMPDH, which is used for E3 ubiquitination and proteasomal degradation [25]. Moreover, a recent study showed that the PSMD14-induced deubiquitination of PKM2 reduces its enzymatic activity; this also promotes the nuclear localization of PKM2, induces the expression of downstream cancer-promoting genes, and consequently drives the malignant progression of

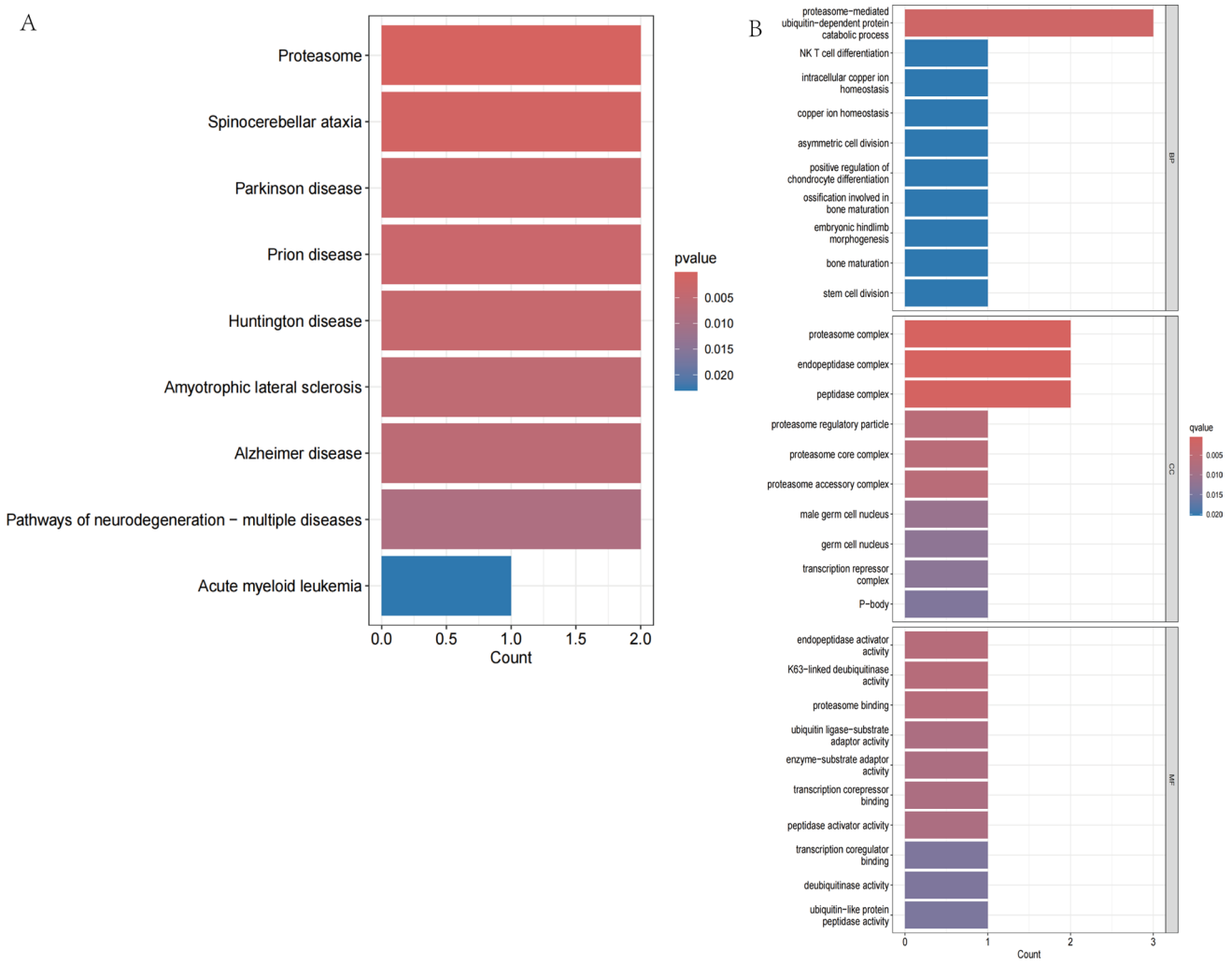

Fig. 8 Differential gene studies using GO and KEGG. **A** The differential gene KEGG enrichment analysis histogram. **B** A histogram showing the differential genes' GO enrichment analysis

ovarian cancer [26]. Islr regulates insulin sensitivity by interacting with Psma4, resulting in ubiquitin-independent proteasomal degradation of Insrα in obese mice [27]. Low expression of ZBTB16 correlates with better projections in patients with cervical cancer [28], which is in line with the findings of our study. In addition, ubiquitination and degradation of Atg14L has been shown to be regulated by the ZBTB16-Cullin3-Roc1 E3 ubiquitin ligase complex [22, 29]. However, the significance of the other three genes in CESC remains uncertain, which is a direction for future cervical cancer research.

Recently, there has been a lot of interest in the connection between carcinogenesis and E3 ligases, which are necessary for ubiquitination [30]. Targeted protein degradation's growing significance in cancer investigation and therapy [31]. And yet, it is still unclear what regulatory mechanisms could potentially be at play between cancerous tumors and E3 ligase-induced ubiquitination. Differential genes were found to be part of present in biological processes (BP), molecular functions (MF), and cellular components (CC), consistent with GO and KEGG pathway enrichment studies. In cervical cancer, all three are believed to be enriched coupled with connections to different signal transduction-related pathways.

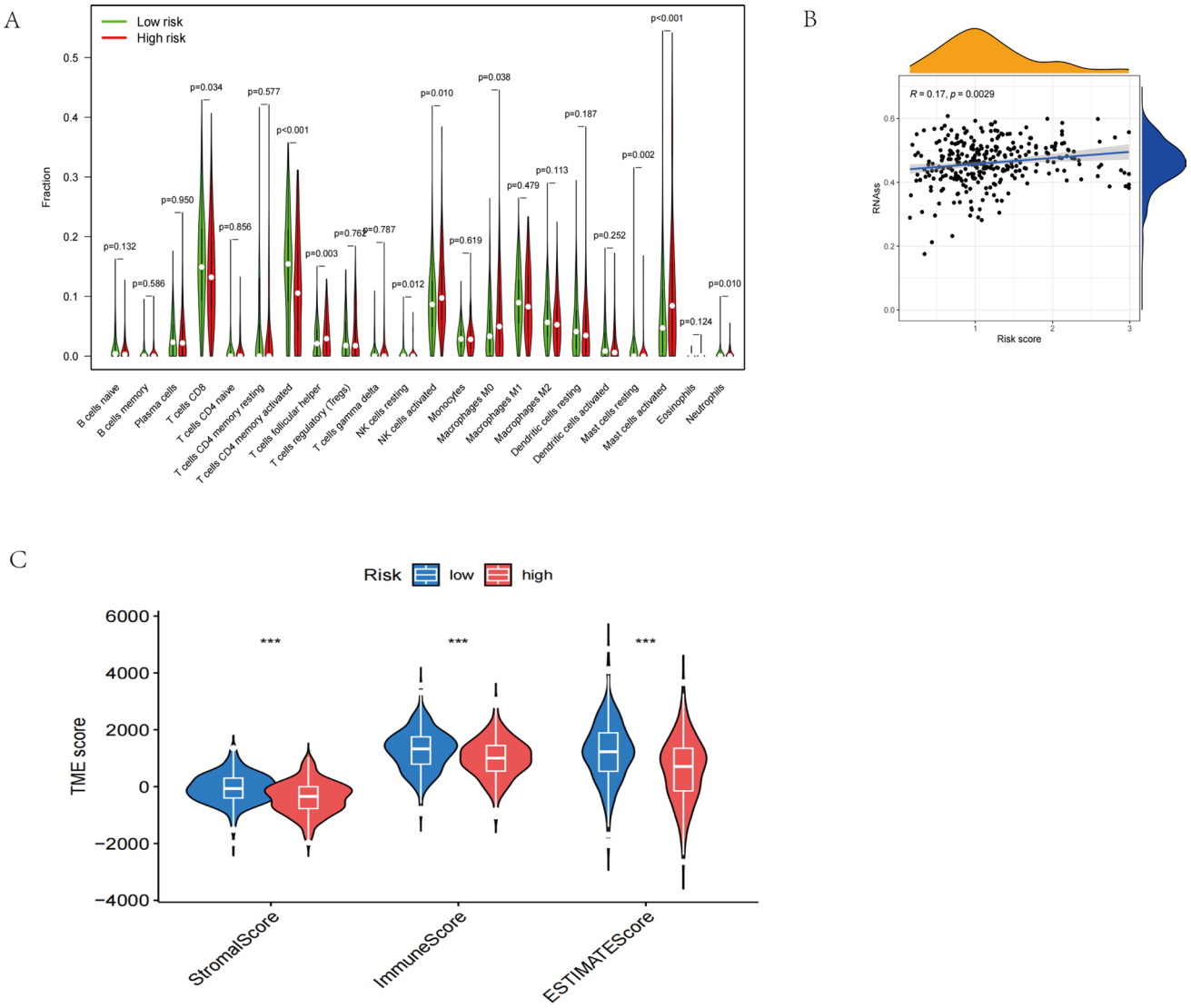

Fig. 9 Variances in the microenvironment of the tumor. **A** The proportion of 22 immune cell subtypes that populate both high- and low-risk individuals. **B** Risk group and stem cell correlation scatter plot. **C** Variations in the two groups' immune microenvironment ratings

We have gained a better grasp of the mechanisms behind the spread of tumors and prognosis in cervical cancer, which is not surprising thinking about the crucial role that E3 ligases play in neoplasia.

In addition, we found that the expression levels of CD8T cells, T cells CD4 memory activated, Mast cells resting and Neutrophils were lower in the high-risk group than in the low-risk group. This certainly suggest that immune cell infiltration and a great prognosis for CC patients are regarding [32]. Interestingly, the immunological barriers score of the low risk group was significantly greater than that of the lowest risk group. This indicates that the notable tumors immune intrusion was not fully exploited as well as that the anti-tumor action of immune cells was inhibited in this group of cells. That means the excellent outcome in patients with low-risk cervical cancer may be understood by their optimized immunity against the disease.

However, there are certain limitations to our investigation. Case selection bias may occur because all samples were retrieved retrospectively and the great majority of analyses employed data from datasets that were made publically available. To validate our preliminary findings, more in vitro and in vivo studies are required.

In conclusion, we designed a molecular cluster and prognostic signature based on E3URGs, which can help predict survival, guide immunotherapy and determine clinical outcomes. This study has the potential to provide deeper insights into the function of ubiquitinated E3 ligases in CESC and facilitate the development of more effective therapies for this disease.

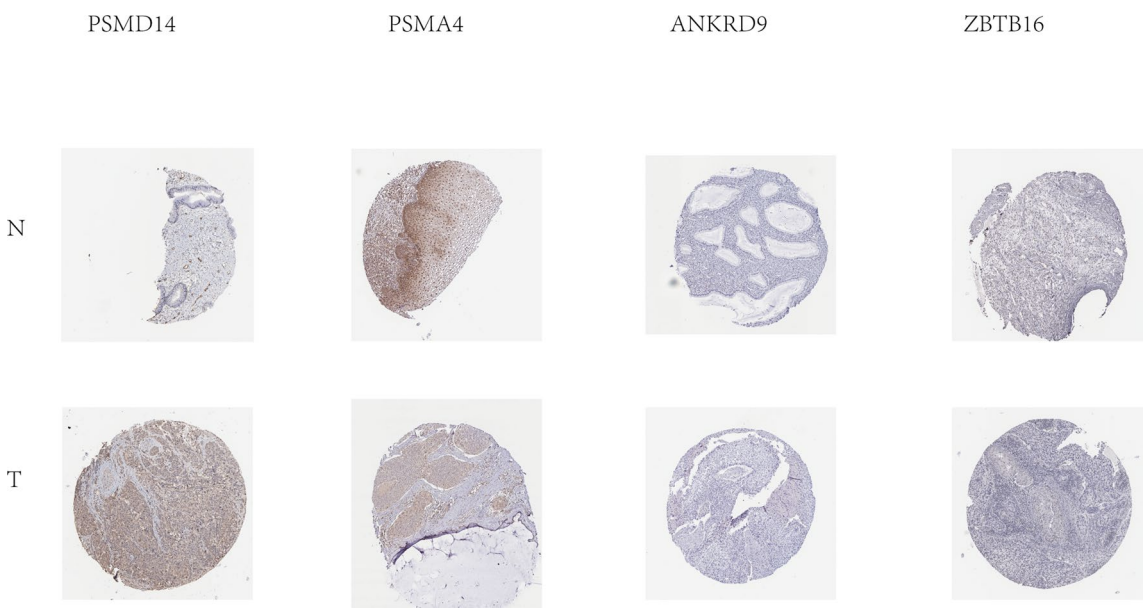

Fig. 10 Using the HPA database, four prognostic genes' protein expression have been investigated

Acknowledgements Not applicable.

Author contributions Zhengchao Yan:Conceptualization,Investigation, Methodology, Data curation,Visualization, Writing -original draft.Jingwei Yu,Shuyuan Wang: Investigation, Methodology,Resources.Weibo Wen, Mengyuan Xin: Investigation,Formal analysis. Funding acquisition. Xiangdan Li: Writing—Review & Editing,Supervision,Project administration, Funding acquisition.

Funding This research was supported by the National Natural Science Foundation of China (No. 82360479); Natural Science Research Foundation of Jilin Province for Sciences and Technology (YDZJ202301ZYTS205).

Data availability The datasets presented in this study can be found in online repositories or coresponding author after the requestion. The names of the repository/repositories and accession number(s) can be found in the article.

Declarations

Competing interests The authors declare no competing interests.

References

1. Qu X, et al. Identification of a novel six-gene signature with potential prognostic and therapeutic value in cervical cancer. Cancer Med. 2021;10(19):6881–96.
2. Bray F, et al. Global cancer statistics 2018: GLOBOCAN estimates of incidence and mortality worldwide for 36 cancers in 185 countries. CA Cancer J Clin. 2018;68(6):394–424.
3. Ayen A, Jimenez Martinez Y, Boulaiz H. Targeted gene delivery therapies for cervical cancer. Cancers. 2020. https://doi.org/10.3390/cancers12051301.
4. Woodman CB, Collins SI, Young LS. The natural history of cervical HPV infection: unresolved issues. Nat Rev Cancer. 2007;7(1):11–22.
5. Rajaram S, Gupta B. Screening for cervical cancer: Choices & dilemmas. Indian J Med Res. 2021;154(2):210–20.
6. Volkova LV, Pashov AI, Omelchuk NN. Cervical carcinoma: oncobiology and biomarkers. Int J Mol Sci. 2021. https://doi.org/10.3390/ijms222212571.

7. Zhai F, et al. The E3 ligases in cervical cancer and endometrial cancer. Cancers (Basel). 2022. https://doi.org/10.3390/cancers14215354.
8. Atri Y, et al. CUL4A silencing attenuates cervical carcinogenesis and improves Cisplatin sensitivity. Mol Cell Biochem. 2024;479(5):1041–58.
9. Maeda R, et al. TBP-like protein (TLP) disrupts the p53-MDM2 interaction and induces long-lasting p53 activation. J Biol Chem. 2017;292(8):3201–12.
10. Hayden MS, Ghosh S. Shared principles in NF-kappaB signaling. Cell. 2008;132(3):344–62.
11. Lee MS, et al. PI3K/AKT activation induces PTEN ubiquitination and destabilization accelerating tumourigenesis. Nat Commun. 2015;6:7769.
12. Hao HX, et al. ZNRF3 promotes Wnt receptor turnover in an R-spondin-sensitive manner. Nature. 2012;485(7397):195–200.
13. Liu K, et al. Stabilization of TGF-beta receptor 1 by a receptor-associated adaptor dictates feedback activation of the TGF-beta signaling pathway to maintain liver cancer stemness and drug resistance. Adv Sci. 2024. https://doi.org/10.1002/advs.202402327.
14. Brodermann MH, Henderson EK, Sellar RS. The emerging role of targeted protein degradation to treat and study cancer. J Pathol. 2024;263(4–5):403–17.
15. Ostertag MS, et al. Structural insights into BET client recognition of endometrial and prostate cancer-associated SPOP mutants. J Mol Biol. 2019;431(11):2213–21.
16. Benowitz AB, Jones KL, Harling JD. The therapeutic potential of PROTACs. Expert Opin Ther Pat. 2021;31(1):1–24.
17. Yu Y, et al. Construction of a CCL20-centered circadian-signature based prognostic model in cervical cancer. Cancer Cell Int. 2023;23(1):92.
18. Salmena L, et al. A ceRNA hypothesis: the rosetta stone of a hidden RNA language? Cell. 2011;146(3):353–8.
19. Zhou RS, et al. Integrated analysis of lncRNA-miRNA-mRNA ceRNA network in squamous cell carcinoma of tongue. BMC Cancer. 2019;19(1):779.
20. Gao Y, et al. Construction and assessment of a prognostic risk model for cervical cancer based on lactate metabolism-related lncRNAs. Int J Gen Med. 2023;16:2943–60.
21. Zheng G, et al. The clinical significance and immunization of MSMO1 in cervical squamous cell carcinoma based on bioinformatics analysis. Front Genet. 2021;12: 705851.
22. Nakayama KI, Nakayama K. Ubiquitin ligases: cell-cycle control and cancer. Nat Rev Cancer. 2006;6(5):369–81.
23. Teixeira LK, Reed SI. Ubiquitin ligases and cell cycle control. Annu Rev Biochem. 2013;82:387–414.
24. Li D, et al. GFPT1 promotes the proliferation of cervical cancer via regulating the ubiquitination and degradation of PTEN. Carcinogenesis. 2022;43(10):969–79.
25. Lee Y, et al. ANKRD9 is associated with tumor suppression as a substrate receptor subunit of ubiquitin ligase. Biochim Biophys Acta Mol Basis Dis. 2018;1864(10):3145–53.
26. Wang, Y., et al., Deubiquitinase PSMD14 promotes tumorigenicity of glioblastoma by deubiquitinating and stabilizing beta-catenin. Biofactors, 2024.
27. Deng Y, et al. Anti-HPV16 oncoproteins siRNA therapy for cervical cancer using a novel transdermal peptide PKU12. Front Oncol. 2023;13:1175958.
28. Zhang T, et al. G-protein-coupled receptors regulate autophagy by ZBTB16-mediated ubiquitination and proteasomal degradation of Atg14L. Elife. 2015;4: e06734.
29. Wang QQ, et al. Hyperthermia promotes degradation of the acute promyelocytic leukemia driver oncoprotein ZBTB16/RARalpha. Acta Pharmacol Sin. 2023;44(4):822–31.
30. Su D, et al. E3 ubiquitin ligase RBCK1 confers ferroptosis resistance in pancreatic cancer by facilitating MFN2 degradation. Free Radic Biol Med. 2024;221:136–54.
31. Li H, et al. Wedelolactone suppresses breast cancer growth and metastasis via regulating TGF-beta1/Smad signaling pathway. J Pharm Pharmacol. 2024;76(8):1038–50.
32. Kim SY, et al. Lyophilizable and multifaceted toll-like receptor 7/8 agonist-loaded nanoemulsion for the reprogramming of tumor microenvironments and enhanced cancer immunotherapy. ACS Nano. 2019;13(11):12671–86.